Comparative Quantitative Proteomic Analysis Reveals Differentially Expressed Proteins Involved in Grain-Filling Rate of Rice at the Early Ripening Stage

Jiana Chen
Hunan Agricultural University
Fangbo Cao
Hunan Agricultural University
Min Huang
Hunan Agricultural University
Salah Fatouh Abou-Elwafa (elwafa75@aun.edu.eg)
Assiut University Faculty of Agriculture https://orcid.org/0000-0002-9018-598X

Research article

Keywords: Rice, Proteomics, grain filling, LC-MS/MS analysis, TMT labeling, Differential protein expression

Posted Date: June 10th, 2020

DOI: https://doi.org/10.21203/rs.3.rs-30611/v1

Abstract

Background

Grain-filling ability is a determinant factor of rice potential yield. Grain filling is a biological process of starch accumulation involved a large number of major enzymes implicated in carbohydrates metabolism in developing rice endosperm and is governed by a complex balance between the sink (grains) and the source (assimilates). This study was carried out to analyze the proteomic profile of rice grains and to identify proteins associated with high grain-filling rate during the early ripening period in rice.

Results

TMT and LC-MS/MS were employed in analyzing proteomic profile of grains from two rice cultivars possess contrasting phenotypes in grain filling rate to identify proteins associated with high grain-filling rate during the early ripening stage. The two cultivars differed significantly in grain-filling rate during the period of 0–3 days after full heading, indicating the appropriacy of cultivars selection for quantitative proteomic analysis. A total of 219 differentially expressed proteins in grains between the two cultivars were identified, providing a database for quantified proteomics in rice grains during grain filling stage. Elevated expression of many enzymes involved in starch and sucrose metabolism during rice grain filling was observed. GO and KEGG analyses revealed that the largest portion of differentially expressed proteins during grain filling associated with carbohydrate metabolism and transportation, suggesting a more specific function of those protein in rice grain development. Starch, sucrose, fatty acids and amino acids biosynthesis and metabolism were significantly enriched pathways.

Conclusions

Analysis of protein-protein interactions indicated the implication of the same proteins in several biological processes such as carbohydrate transport and metabolism, fatty acid metabolism, energy production and conversion and secondary metabolites biosynthesis. The data provide valuable information about the roles of biosynthesis, transport and metabolism of carbohydrate and amino acids in rice grain filling and development. The results represent a valuable foundation for further studies of the roles of differentially expressed proteins in underlying grain filling stage in rice and their potential impacts on rice productivity.

Background

Rice (*Oryza sativa* L.) is one of the most crucial food crop worldwide, in particular in Asia and the Pacific region, therefore improving rice productivity is of great importance to meet the rapid population growth and economic development and to ensure sustainable human food and animal feeding [1]. Grain yield which is one of the essential yield component parameters is defined as the product of yield sink capacity

and filling efficiency [2]. Grain-filling is a pivotal grain weight determinant factor and has a great impact on rice potential yield. High yielding rice cultivars that have been developed in many rice producing countries are characterized by having extra-large sink capacity but differed greatly in grain-filling ability [3, 4]. Although both grain-filling rate and duration are associated with grain weight, high grain weight was attributed to a high grain-filling rate [5]. Although high yielding rice cultivars that have large panicles or/and extra heavy panicles with a large number of spikelets per panicle have become available, e.g., the New Plant Type, hybrid rice and 'super' rice [4, 6, 7], those cultivar however and due to their poor grain-filling do not reach their high yield potential

Grain filling is governed by a complex balance between the sink (grains) and the source (assimilates; [4]). Modern high yielding rice cultivars with large panicle have a large sink capacity, however the insufficient carbohydrate source and export might cause poor filling capacity of inferior spikelet, reduce the rate of seed setting and ultimately reduce grain yield [2]. On the other hand, efficient coordination of source capacity (assimilates), efficiency of carbohydrate transport (flow) and sink activity are crucial factors in increasing grain-filling rate and hence increasing rice yields [8, 9]. Photoassimilates and the nonstructural carbohydrates (NSCs) stored in the culms and sheaths before heading are the most important source for assimilated carbon molecules during rice grain-filling [10, 11]. Enhancing NSCs accumulation in culms as well as their transportation to rice grains improve sink capacity, grain-filling rate, and grain yield [2, 11]. Therefore, it is of great immense to dissect the molecular mechanisms of culm NSCs accumulation and transportation to maximize rice yield potentials. Unloading sugars to grains during grain filling is affected by plant photosynthetic capacity and the efficiency of NSCs flow from the culms to the panicle. However, the abundance of NSCs enhances the sink activity and promotes grain filling at the early stage of grain-filling [10]. Transportation of sucrose from the source to the sink is influenced by 3 factors, i.e., phloem loading, length of transportation distance and phloem unloading. Transportation of assimilates from the source to the sink is influenced by the function and structure of the vascular bundles, including the size, number, development and capacity flow of the bundles [12]. Environmental factors that reduce photosynthetic capacity and thereby affect the accumulation and transportation of culm NSCs such as heat stress, water deficit, low radiation level and nutrient deficiency enhances the transportation of culm NSCs [13–16].

Starch, contributes up to 80–90% of the dry weight of unpolished rice grains, is the main NSCs storage form in the sheaths and culms and accumulates during the vegetative growth period of rice plants and reduced sharply during grain-filling [17, 18]. Culm NSCs contributed up to 10–40% of grain yield in rice, however great variations among rice cultivars in the accumulation of NSCs in the culms and their transportation to the grains have been observed [2, 19].

At the molecular level, grain-filling is a biological process of starch accumulation involving an estimated number of 33 major enzymes implicated in carbohydrates metabolism in developing rice endosperm [20], five of which, i.e., sucrose synthase, invertase (β-fructofuranosidase), adenosine diphosphate-glucose pyrophosphorylase (AGPase), starch synthase and starch branching, have been reported to underly starch synthesis during starch accumulation in rice culms prior to heading [13, 20, 21]. However, after heading,

culms starch is the first compound of NSCs to be converted to sucrose which is the primary sugar transported from. The enzymes implicated in sucrose synthesis and degradation regulate culms sucrose content and transportation of NSCs from culms to developing grains post-anthesis [22]. Starch metabolism and degradation occur through hydrolytic and phosphorolytic reactions and might be a result of collaborative action of several enzymes [23, 24]including α-amylase (1,4-α-D-glucan glucanohydrolase), β-amylase (1,4-α-D-glucan maltohydrolase, α-glucosidase (α-D-glucoside glucohydrolase, and starch phosphorylase (1,4 α-D-glucan:orthophosphate α-D-glucosyltransferase) [25]. Accordingly, the enzyme sucrose-phosphate synthase (6-phosphate-fructose-glycosyltransferase) is anticipated to play an essential role in sucrose re-synthesis [26], and sustaining the assimilatory carbon flux from source to sink [27].

Although, the findings of previous studies are clearly helpful in understanding the physiological basis of grain filling in rice, however more efforts are essentially needed to further dissect the molecular mechanisms underlying grain-filling in rice. Therefore, the current study was conducted to analyze the proteomic profile of rice grains and to identify proteins associated with high grain-filling rate during the early ripening period in rice.

Results

Analysis of grain filling rate

The results showed that the cultivar Xiangzaoxian 42 significantly surpassed the cultivar Xiangzaoxian 24 in grain-filling rate. The grain-filling process was well fitted by the logistic equation for both cultivars, showing a determination coefficient (R^2) of 0.991 and 0.987 for Xiangzaoxian 24 and Xiangzaoxian 42, respectively (Fig. 1a). The grain-filling rate, calculated according to the logistic equations, was more than 2.0 times higher in Xiangzaoxian 42 than in Xiangzaoxian 24 during the period of 0–3 days after full heading (Fig. 1b).

Protein profiles revealed differentially expressed proteins between the two rice cultivars during the early grain filling stage

To further uncover the molecular mechanisms underlying deferential the early grain filling period in the two rice cultivars, i.e., Xiangzaoxian 24 and Xiangzaoxian 42, TMT and LC-MS/MS were employed to characterize the proteomic profiles of grains during the early ripening period (3 days after full heading) of both. Quality control filtering resulted in a total of 8143 and 6808 highly reproduceable proteins that could be quantified in the Xiangzaoxian 24 and Xiangzaoxian 42 cultivars, respectively, that were implemented in the analysis of differentially abundant proteins during the early period of grain filling. Protein profiling analysis identified 219 differentially expressed proteins in grains between Xiangzaoxian 24 and Xiangzaoxian 42 at 3 days after full heading. The molecular weight of those proteins ranged

between 5.51-123.03 kDa. Number of peptides for each protein ranged between 1–27 peptides. Out of those 219 differentially expressed proteins, 112 were up-expressed in the cultivar Xiangzaoxian 24 and down-expressed in the cultivar Xiangzaoxian 42, while the remaining 107 proteins were down expressed in the cultivar Xiangzaoxian 24 and up-expressed in the cultivar Xiangzaoxian 42 (Supp. Table 1). The down- and up-expression ratio of the differentially expressed proteins ranged between 0.11–55.55.

GO and KEGG annotations of deferentially expressed proteins

All deferentially expressed proteins were annotated to the Gene Ontology (GO) database and classified based on their biological process, cellular compartment and molecular function to the GO database. Deferentially expressed proteins covered all three functional categories, i.e., biological process (BP), cellular compartment (CC) and molecular function (MF) (Fig. 2).

The BP category mostly involves metabolic processes, cellular processes, and single-organism process. Proteins with differential abundance levels assigned to CC category are mainly implicated in catalytic activity and binding. The most prominent proteins in the MF category includes cell, membrane and organelle (Fig. 2).

Analysis of the biological metabolic pathways of the 219 differentially expressed proteins using the KEGG databases revealed that those proteins are mainly associated with general function prediction (20), post-translational modifications, protein turnover, chaperons (17), energy production and conversion (12), carbohydrate transport and metabolism (12) and secondary metabolites biosynthesis, transport and catabolism (9) (Fig. 3). Comparison between the two cultivars in terms of differential expression of proteins involved in carbohydrate transport and metabolism and secondary metabolites biosynthesis indicated that they are detected in the Xiangzaoxian 42 cultivar regarding biological process (Suppl. Table 1).

Functional enrichment of differentially expressed proteins

After classification of differentially abundant proteins into different categories, the -log10 (P-value) approach was employed to determine their quantities. According to subcellular location, proteins exhibited increased expression during the early ripening period of grain filling stage are mainly enriched in the chloroplasts, cytoplasm, nucleus, mitochondria and plasma membrane, while proteins exhibited downregulated expression are mainly enriched in chloroplast, cytoplasm, extracellular compartments, mitochondria, nucleus and plasma membrane (Fig. 3; Supp. Table 1).

Classification of the identified proteins based on subcellular location

Subcellular localization annotation was implemented to determine the abundance of differentially expressed proteins in each subcellular location (Fig. 4; Supp. Table 1). Proteins associated with chloroplasts, cytoplasm and nucleus were mainly induced during the early ripening period of grain filling

in rice. Noteworthy, differential expression of proteins was detected in the plasma membrane, extracellular compartment and mitochondria as well during the grain frilling period. Subcellular localization indicated that 1, 2, 3, 3, 10, 10, 14, 36, 48 and 92 differentially expressed proteins are localized to the vacuolar membrane, endoplasmic reticulum, cytoskeleton, peroxisome, mitochondria, plasma membrane, extracellular compartment, nucleus, cytoplasm and chloroplast, respectively. Protein domain analysis indicated that Alpha/Beta hydrolase fold, Glycoside hydrolase superfamily and Glycoside hydrolase, catalytic domains were the top three upregulated protein domain groups where they mapped 8,7 and 6 proteins, respectively. Meanwhile, for the downregulated proteins, START-like and aspartic peptidase domains were the most abundant groups (Fig. 5).

Functional enrichment-based clustering

The KEGG pathways enrichment analysis of differentially expressed proteins identified 22 significantly enriched pathways were identified in the highly expressed proteins including starch and sucrose metabolism, galactose metabolism, fatty acid biosynthesis, fatty acid elongation, MAPK signaling pathway plant, fructose and mannose metabolism, amino acids metabolism, Cyanoamino acid metabolism, oxidative phosphorylation. Likewise, 22 significantly enriched pathways in the low expressed proteins including starch and sucrose metabolism, glycolysis, biosynthesis of secondary metabolites, glycerophospholipid metabolism, pantothenate and CoA biosynthesis, pyruvate metabolism, amino sugar and nucleotide sugar metabolism and amino acids (purine, pyrimidine, glycine, serine, threonine, arginine, proline, tryptophan and glutathione) metabolism (Fig. 6; Supp. Table 1).

To further identify specific protein families, protein functional domain clustering of the previously identified differentially expressed proteins were analyzed. Proteins with decreased expression levels are enriched in RmlC-like cupin, Zinc finger UBP-type, AMP-binding enzyme C-terminal, START-like, Lysozyme-like and Catalase-like domains. Meanwhile, proteins with elevated expression levels are enriched in NAD(P)-binding, Glycoside hydrolase superfamily, Glycoside hydrolase-catalytic, FAE1/Type III polyketide synthase-like, AMP-binding enzyme C-terminal, NmrA-like, Pyruvate/Phosphoenolpyruvate kinase-like, Glutathione S-transferase, Lysozyme-like, Isopenicillin N synthase-like, Non-haem dioxygenase N-terminal and Alpha/Beta hydrolase fold domains (Fig. 7; Supp. Table 1).

According to transformed *Z* score, quantile-based analysis classified proteins into four groups

(Q1, Q2, Q3, and Q4) when ranked by -log10 (P-value). Each quantified protein was then assigned to the respective quantile. Accordingly, quantified proteins were allocated to four quantiles Q1 (> 1.3), Q2 (1.2–1.3), Q3 (1/1.2), and Q4 (< 1/1.3) (Fig. 8a&b). Q1 proteins group are enriched in the hydrolase activity acting on glycosyl bonds of the MF protein category. The Q2 proteins are enriched in the lipid transport of BP protein category, and metal ion binding and cation binding of the MF protein category. Proteins belong to the Q3 group are enriched in formaldehyde catabolic process and hexose metabolic process of the BP protein category, and transferase activity, transferring glycosyl group, S-formylglutathione hydrolase

activity and ATP-phosphoribosyl transferase activity of the MF protein category. However, the Q4 group of proteins are enriched in regulation of proteolysis and negative regulation of hydrolase activity of the BP protein category and peptidase inhibitor activity, peptidase regulator activity, ADP binding, endopeptidase regulator activity, endopeptidase inhibitor activity, enzyme inhibitor activity, enzyme regulator activity and molecular function regulator of the MF protein category (Fig. 8a&b).

KEGG pathway clustering for four protein groups (Q1, Q2, Q3, and Q4) was also carried out (Fig. 8d). Q1 proteins group are enriched in the Ubiquinone and other terpenoid-quinone biosynthesis KEGG pathway. The Q2 proteins group are enriched in the Pentose and glucuronate interconversions and biosynthesis of secondary metabolites pathways. The Q3 proteins group are enriched in the biosynthesis of secondary metabolites pathway. However, no KEGG pathways assigned to the Q4 proteins group (Fig. 8c).

Protein domain-based clustering revealed that the Q1 group of proteins are enriched in Bifunctional inhibitor/plant lipid transfer, START-like, Glycoside hydrolase superfamily and Glycoside hydrolase catalytic domains. The Q2 proteins group are enriched in Mitochondrial carrier, Carboxyl transferase and Bifunctional inhibitor/plant lipid transfer domains. The Q3 proteins are enriched only in the Alpha/Beta hydrolase fold domain. However, proteins of the Q4 group are enriched in Alpha/Beta hydrolase fold domain, DUF1618 and Ankyrin repeat-containing domains (Fig. 8d).

Functional protein interaction networks of differentially abundant proteins

The STRING database v10.5 identified 22 functional protein interaction networks, 9 of which are downregulated while the remaining 13 are upregulated (Fig. 9). Seven protein interaction networks are located in the chloroplast, 6 interactions are located in the cytoplasm, 5 interactions are located in the nucleus, 2 interactions are located in the mitochondria and one interaction located in each of cytoskeleton and extracellular compartment (Fig. 8; Table 1). Seven interaction proteins belong to the chloroplast network, including 4 downregulated proteins, i.e., glutathione S-transferase, heterogeneous nuclear ribonucleoprotein A1/A3, small subunit ribosomal protein S17e and Xylanase inhibitor and 3 upregulated proteins, i.e., Glutathione synthase, Transferase CAF17, mitochondrial and Tropinone reductase I. The cytoplasm protein interaction networks comprise one downregulated interaction, i.e., dUTP pyrophosphatase, and 5 upregulated interactions, i.e., peptide chain release factor subunit 1, small subunit ribosomal protein S2e, large subunit ribosomal protein L24e, tyrosine aminotransferase and glycine hydroxymethyl transferase. The nucleus protein interaction networks include two downregulated interactions, i.e., dUTP pyrophosphatase and translation initiation factor 4A, and two upregulated interactions, i.e., translation initiation factor 3 subunit B, large subunit ribosomal protein L19e and large subunit ribosomal protein L27Ae (Fig. 8; Table 1). Additional information regarding functional protein interaction networks are shown in Supp. Table 1.

Discussion

Analysis of proteomics profiles has been demonstrated as a powerful and efficient molecular tool in exploring molecular mechanisms underlying various biological processes in living organisms. However, the efficiency of proteomic analysis in identification of proteins underlying a given biological process greatly depends on the applied proteomics analysis procedure and the experimental system [28–33]. Although proteomic analyses have been widely employed to dissect the molecular basis of variable biological processes in plants, in particular stress tolerance, [29, 32, 34–39]), to the best of our knowledge this is the first comprehensive study conducted to dissect proteins involved in grain filling rate of rice. Seed development in rice is a complex biological process that directly impact potential yield and is regulated by complex regulatory networks involving several transcription factors [40].In the current study, two rice cultivars, i.e., Xiangzaoxian 24 and Xiangzaoxian 42, that possess contrasting phenotypes in grain filling rate during the early ripening period were employed in identification of grain filling differentially expressed proteins. Determination coefficients (R^2) of the grain-filling process in Xiangzaoxian 24 and Xiangzaoxian 42 cultivars as fitted by the logistic regression were 0.991 and 0.987, respectively, suggesting that the logistic regression is a reliable analysis to fit the grain-filling process in rice which is consistent with previous reports [5, 41]. The cultivar Xiangzaoxian 42 exhibited a grain-filling rate during the period of 0–3 days after full heading that is 2-times higher than that of the cultivar Xiangzaoxian 24 as estimated by the logistic regression, indicating the appropriacy of cultivars selection for quantitative proteomic analysis.

The TMT-labeled quantitative LC-MS/MS proteomics and LC-MS/MS metabolomics that rely on the high-throughput quantitative detection procedure was employed to perform quantitative proteomics analysis of the grain samples harvested from the two rice cultivars 3 days after heading. Quality control filtering identified a total of 8,143 and 6,808 highly reproduceable proteins that were quantified in the Xiangzaoxian 24 and Xiangzaoxian 42 cultivars, respectively, and were implemented in the analysis of differentially expressed proteins. The TMT procedure is a powerful approach in quantitative proteomic analysis offering higher sensitivity for the analysis [36]. Through annotation and identification of differentially expressed proteins, the key genes/proteins and pathways underlying the early period of grain filling stage in rice were dissected. The analysis aimed to obtain a more comprehensive understanding of the alterations of grain composition in terms of protein profiling during the early ripening period of grain filling between the two phenotypically contrasting cultivars, and hence further exploring molecular mechanism underlying rice yield. Further bioinformatics analyses uncovered crucial proteins for the metabolic network and their regulation during the early period of grain filling stage. These findings represent a theoretical basis required for dissecting molecular mechanisms of grain filling and their impact on potential yield. Revealing the abundance of protein expression during grain filling provides essential information on grain formation and development, and the accumulation of starch as well as improving crop productivity. Our data revealed the elevated expression of many enzymes involving in starch and sucrose metabolism during rice grain filling. The results of GO and KEGG analyses revealed that the largest portion of differentially expressed proteins during grain filling associated with metabolism. Most of these proteins are implicated in the transportation and metabolism of carbohydrate, production and conversion of energy, biosynthesis and transportation of secondary metabolites, and

catabolism and metabolism of amino acids (Fig. 3; Supp. Table 1). Besides, most of those proteins are differentially expressed between the two cultivars during grain filling, indicating that the enhancement of the primary metabolism to facilitate grain filling which is consistent with previous studies [42–46] that revealed that the upregulation of metabolic proteins enhances seed development. The abundance of some metabolic proteins in plants such as those involved in glycolysis, carbohydrate metabolism and amino acid synthesis may reflect enhanced plant growth and development [47, 48]. Our data showed that proteins involved in glycolysis and carbohydrate metabolism (e.g., Glycoside hydrolase superfamily, Xyloglucan endotransglucosylase/hydrolase, Starch synthase, chloroplastic/amyloplastic, Mannose-6-phosphate isomerase and Glycoside hydrolase superfamily; Suppl. Table 2) are among the most differentially regulated proteins during the early stage of grain filling, suggesting a more specific function of those protein in grain development. It was further shown that amino acid metabolism proteins which are essential for seed coat, endosperm formation and embryo are among the most highly regulated in rice grains. Several proteins involved in transport, storage, stress tolerance and defense (e.g., glucose 1 phosphate adenyltransferase, heat shock proteins, MAPK signaling, pathogenesis-related protein PRB1, granule bound starch synthase, β amylase, etc.) exhibited differential expression patterns during grain filling which is consistent with previous finding in other crop plants, suggesting a biological function of those proteins in rice grain filling [34, 35].

According to the KEGG pathway enrichment analysis, fatty acid biosynthesis, fructose and mannose metabolism, glutathione metabolism, starch and sucrose metabolism, biosynthesis of secondary metabolites and amino acids biosynthesis and metabolism were significantly enriched pathways (Fig. 6; Supp. Table 2). The synthesis, metabolism and transport of carbohydrates and amino acids which play crucial roles in starch and protein accumulation were enhanced to promote grain filling and to accelerate conversion rate between different substances [34, 35, 49]. Besides. analysis of domain enrichment of proteins exhibited that Alpha/Beta hydrolase fold, Glycoside hydrolase superfamily, Glycoside hydrolase, catalytic domain, START-like and Aspartic peptidase were the top protein domain groups with different dynamic expression patterns (Fig. 7).

To provide an effective approach for dissecting the molecular mechanisms underlying protein expression during the early stage of grain filling, we have employed the online tool STRING 10.5 database to obtained protein-protein interaction (PPI) information. The central nodes in directed and undirected PPI networks represent individual proteins, and the lines show their relationships. The degree and combined score between each two nodes were implemented to estimate the nodes of differentially expressed protein-derived interaction networks. Analysis of protein-protein interaction indicated that the same proteins might implicated in several biological processes such as carbohydrate transport and metabolism, fatty acid metabolism, energy production and conversion and secondary metabolites biosynthesis.

Conclusions

TMT and LC-MS/MS were employed to analyze the proteomic profiles of rice grains during the early ripening stage of two rice cultivars possess contrasting phenotypes in grain filling rate, and to further explore the molecular mechanisms underlying rice grain yield. Protein profiling analysis identified 219 differentially expressed proteins in grains between the two cultivars at 3 days after full heading, providing a database for quantified proteomics in rice grains during grain filling stage. Integrated analysis of proteomic data revealed that deferentially expressed proteins covered the three functional categories, i.e., biological process (BP), cellular compartment (CC) and molecular function (MF), indicating the comprehensiveness of proteomic profiling of our study. GO and KEGG pathway analyses showed that the largest group of differentially abundant proteins are involved in carbohydrate transport and metabolism, energy production and conversion, secondary metabolites biosynthesis, transport and catabolism, and amino acid metabolism, indicating that the enhancement of the primary metabolism to facilitate grain filling. Analysis of functional protein interaction networks revealed that the same proteins were shown to be involved in several biological processes such as carbohydrate transport and metabolism, fatty acid metabolism, energy production and conversion and secondary metabolites biosynthesis. Our data provide valuable information about the roles of biosynthesis, transport and metabolism of carbohydrate and amino acids in rice grain filling and development. Besides, the results of this study represent a valuable foundation for further studies of the roles of differentially expressed proteins in underlying grain filling stage in rice and their potential impacts on rice productivity.

Methods

Plant materials and experiments

Two rice cultivars, i.e., Xiangzaoxian 24 and Xiangzaoxian 42, provided by the Nongfeng Seed Industry Co., Ltd., Changsha, China exhibited contrasting phenotypes in grain filling during the early ripening period were used in the current study. The cultivar Xiangzaoxian 24 exhibited a slower grain filling compared to the cultivar Xiangzaoxian 42 during the early ripening period [5, 41]. The randomized complete-block design with three replicates with a plot size of 40 m^2 were implemented in carrying out a field experiment growing the two cultivars in Yongan (28°09' N, 113°37' E, 43 m asl), Hunan Province, China, in the early rice-growing season in 2018. The soil physical and chemical analyses were performed based on samples taken from the 0–20 cm layer prior to the beginning of the experiment. The basic physical and chemical characteristics of the experimental field soil are shown in Table 2.

Seeds were sown in trays on March 26, 2018 and 25-day-old seedlings were transplanted into the field on April 20using the high-speed rice transplanter (PZ80-25, Dongfeng Iseki Agricultural Machinery Co., Ltd., Xiangyang, China). Transplanting of rice seedlings was done at 25 cm spacing between rows and 11 cm between plants within rows. To ensure a uniform plant population, missing plants were re-transplanted by hand 7 days later. Nitrogen fertilization was applied in three doses: 67.5 kg N ha^{-1} as basal fertilizer (a day prior to transplanting), 27.0 kg N ha^{-1} at early-tillering (7 days post transplanting), and 40.5 kg N ha^{-1} at panicle initiation. Phosphorus fertilization of 67.5 kg P_2O_5 ha^{-1} was applied as a basal fertilizer

dose. Potassium fertilization of 135 kg K_2O ha^{-1} was equally split between the basal fertilization dose and panicle initiation fertilization dose. The experiments were kept under flooded conditions from transplanting until 7 days before maturity. Chemical treatments were applied to control diseases, insects, and weeds.

Protein extraction

Three days after heading, 3 tagged panicles from each plot were sampled for protein extraction. The grains in the middle part of the sampled panicles were hand threshed, frozen in liquid nitrogen for 1 min, and stored at − 80 °C until assayed.

After grain sample was grinded in liquid nitrogen it has been transferred to a 5-ml centrifuge tube. After grinding, lysis buffers, i.e., 8 M urea, 10 mM dithiothreitol, 1% Triton-100, and 1% Protease Inhibitor Cocktail were added to the cell powder, followed by sonication on ice for three times using a high intensity ultrasonic processor (Scientz). Centrifugation at 20,000 g at 4 °C for 10 min was carried out to remove the remaining debris. The protein was precipitated with cold 20% TCA for 2 h at -20 °C. After centrifugation at 12,000 g 4 °C for 10 min, the supernatant was discarded. Cold acetone was then used to wash the remaining precipitate for three times. The protein was dissolved in 8 M urea and its concentration was estimated using BCA kit according to the manufacturer's instructions.

Trypsin digestion and TMT labeling

Samples digestions were performed according to the procedure described previously [29]. In brief, a 5 mM dithiothreitol was applied for 30 min at 56 °C to reduce protein solution. After alkylation using mM iodoacetamide for 15 min at room temperature in dark, 100 mM TEAB was used to dilute protein samples. Trypsin was added for the first digestion at mass ratio of 1:50, trypsin:protein, overnight, and at mass ratio of 1:100, trypsin:protein, for the second digestion for 4 h. Strata X C18 SPE column (Phenomenex) followed by vacuum-dried was used to desalt peptide. Reconstitution of peptide was performed in 0.5 M TEAB and employed based on the TMT kit manufacturer's procedure. After incubation of peptide mixtures for 2 h, vacuum centrifugation at room temperature was performed for desalination and drying.

Protein fractionation and identification using LC-MS/MS analysis

The Agilent 300Extend C18 column in the high pH reverse-phase HPLC was employed in fractionation of tryptic peptides. A gradient concentration of 8–32% of acetonitrile (pH 9.0) was then applied for 60 min to separate peptides into 60 fractions. Afterwards, peptides were combined in 18 fractions and dried using vacuum centrifuging. After dissolving the tryptic peptides were in 0.1% formic acid (solvent A), they were loaded onto a reversed-phase analytical column (15-cm length, 75 μm i.d.). The gradient was composed of an increase from 6–23% solvent B (0.1% formic acid in 98% acetonitrile) over 26 min, 23–35% in 8 min and climbing to 80% in 3 min then remain at 80% for the last 3 min, all at a constant flow rate of 400 nL/min on an EASY-nLC 1000 UPLC system.

After exposing peptides to NSI source, the Q ExactiveTM Plus (Thermo Fisher Scientific, Waltham, MA, USA) was implemented for tandem mass spectrometry (MS/MS). The electrospray applied voltage was 2.0 kV. The m/z scan range was at 350 to 1800 for full scan, and the Orbitrap was then employed to detect the intact peptides at a resolution of 70,000. MS/MS of peptides was performed using the NCE setting as 28, the Orbitrap was implemented to detect the fragments at a resolution of 17,500. A data-dependent approach that switches between one MS scan and 20 MS / MS scans with a dynamic exclusion of 15.0 seconds. Automatic gain control (AGC) was adjusted to 5E4, and the fixed first mass was adjusted to 100 m/z.

The Maxquant search engine (v.1.5.2.8) was employed in processing the resulting MS/MS data. Tandem mass spectra were searched against *XXX* database linked to reverse decoy database. Trypsin/P is identified as a cleavage enzyme that allows up to 2 missing cleavages. The mass tolerance for the precursor ions was adjusted to 20 ppm in first search and 5 ppm in the main search, and the mass tolerance for the fragment ions was adjusted to 0.02 Da. Carbamidomethyl on Cys was designated as fixed modification and oxidation on Met as variable modifications. FDR was adjusted to < 1% and minimum score for peptides was set > 40.

Proteomic analysis and identification of differentially abundant proteins

Proteomic analysis was performed using PTM BioLab Co., Ltd. (Hangzhou, China), using tandem mass tag coupled to liquid chromatography-mass spectrometry/mass spectrometry. Proteins with relative quantification p-values < 0.05 and fold-changes > 1.30 or < 1/1.30 were selected as differentially expressed. The Kyoto Encyclopedia of Genes and Genomes (KEGG) database was employed to identify differentially expressed proteins related to starch and sucrose metabolism.

Gene ontology (GO), InterPro domain and KEGG pathway annotations and subcellular localization of abundant expressed proteins

Gene Ontology proteome annotation was derived from the UniProt-GOA database (http://www.ebi.ac.uk/GOA/). Identified protein ID was converted into UniProt ID and then mapped to GO IDs by protein ID. The InterProScan soft (http://www.ebi.ac.uk/interpro/, v. 5.14-53.0) that depends on protein sequence alignment approach was performed to annotate functional GO of the previously identified proteins that failed to be annotated to UniProt-GOA database. GO annotation was performed in proteins classification to three categories, i.e., biological process, cellular compartment and molecular function. Using the InterPro domain database, the InterProScan was implemented in annotation of functional description of identified proteins domain based on protein sequence similarity.

Annotation of protein pathways was then performed using the Kyoto Encyclopedia of Genes and Genomes (KEGG) database. Protein description of the KEGG database was annotated using theonline service tools KAAS of the KEGG. The KEGG mapper online service tools of the KEGG was then performed to map the annotation results to the KEGG pathway database. The subcellular protein localization

predication software WolfPSORT (http://wolfpsort.seq.cbrc.jp/) was implemented to predict subcellular localization of differentially abundant proteins.

Enrichment of GO, KEGG pathway and protein domain analyses

GO annotation classified differentially expressed proteins into three categories, i.e., biological process, cellular compartment and molecular function. To test enrichment significancy of differentially abundant proteins against all identified proteins in each category, two-tailed Fisher's exact test was performed. Enrichment was considered significant when the corrected p-value of a given GO is below 0.05. The two-tailed Fisher's exact test was also implemented to further identify significantly enriched pathways in the KEGG database. The pathway with a corrected p-value less than 0.05 was considered significant. The KEGG website classified these pathways into hierarchical categories. The InterPro database was researched and the two-tailed Fisher's exact test was also performed to identify the significancy of enrichment of the differentially abundant proteins in each protein category. Protein domains with a p-value below 0.05 were considered significant.

Enrichment and quantiles-based clustering

For further hierarchical clustering based on different protein functional classification, e.g., GO, Domain, Pathway and Complex. All protein categories obtained after enrichment along with their P values were collated. Categories that are enriched in at least one of the groups with a P value below 0.05 were filtered. The mean (x) and standard deviation (y) of the -log10 (P-value) of all quantified proteins was estimated. Transformation of the P-value ratios of quantified proteins to Z scores according to the function X = −log10 (P-value) was employed. Z-transformation of these X values was performed for each functional category. The one-way hierarchical clustering tool (Euclidean distance, average linkage clustering) in Genesis was implemented in clustering the Z scores. The "heatmap.2" function in the "gplots" R-package was employed to generate cluster memberships that were visualized by a heat map.

Protein-protein interaction network

The accession and sequence databases of differentially expressed protein were queried against the STRING database v 10.5 for protein-protein interactions. Only the interactions between the proteins belonging to the queried dataset were considered, thus external candidates were excluded. The "confidence score" metric in the STRING database was implemented to define the confidence of interaction. Interactions of a confidence score > 0.7 (high confident) were selected. The "networkD3" function in the R package was employed to visualize the Protein-protein interaction network form the STRING database.

Statistical analysis

A three replicate experimental design was followed for all experiments. The analysis of variance (ANOVA) in the R package was employed to statistically analyze all estimated parameters, e.g, GO functional enrichment and KEGG pathway.

Abbreviations

NSCs
nonstructural carbohydrates
AGPase
adenosine diphosphate-glucose pyrophosphorylase
R2
determination coefficient
kDa
kilodaltons
GO
Gene Ontology
BP
biological process
CC
cellular compartment
MF
molecular function
KEGG
The Kyoto Encyclopedia of Genes and Genomes
PPI
protein-protein interaction
ANOVA
analysis of variance

Declarations

Ethics approval and consent to participate

Not applicable.

Consent for Publication

Not applicable.

Availability of data and material

All data are included within the manuscript and its supplementary material.

Competing interests

The authors declare that there is no conflict of interest.

Funding

All experimental work reported in this manuscript was financially supported by the National Key R&D Program of China (2017YFD0301503).

Authors' contributions

MH conceived the study, analyzed the data, and wrote the manuscript. JC and FC performed the experiment and collected the data. SFA analyzed the data and wrote the manuscript. All authors read and approved the final version of the manuscript.

Acknowledgments

This work was financially supported by the National Key R&D Program of China (2017YFD0301503). The authors thank those who have been at the forefront of the fight against the 2019 novel coronavirus for allowing us to have peace of mind to concentrate on writing this manuscript.

References

1. Li K, Yu H, Li T, Chen G, Huang F. Cadmium accumulation characteristics of low-cadmium rice (Oryza sativa L.) line and F1 hybrids grown in cadmium-contaminated soils. Environ Sci Pollut Res. 2017;24(21):17566–76.
2. Yang J, Zhang J. Grain-filling problem in ‘super’ rice. J Exp Bot. 2009;61(1):1–5.
3. Yoshinaga S, Takai T, Arai-Sanoh Y, Ishimaru T, Kondo M. Varietal differences in sink production and grain-filling ability in recently developed high-yielding rice (Oryza sativa L.) varieties in Japan. Field Crops Research. 2013;150:74–82.
4. Okamura M, Arai-Sanoh Y, Yoshida H, Mukouyama T, Adachi S, Yabe S, Nakagawa H, Tsutsumi K, Taniguchi Y, Kobayashi N, et al. Characterization of high-yielding rice cultivars with different grain-filling properties to clarify limiting factors for improving grain yield. Field Crops Research. 2018;219:139–47.
5. Huang M, Zou YB. Comparison of grain-filling characteristics between two super rice cultivars with remarkable difference in grain weight. World Appl Sci J. 2009;6:6.
6. Yang J, Peng S, Zhang Z, Wang Z, Visperas RM, Zhu Q. Grain and Dry Matter Yields and Partitioning of Assimilates in Japonica/Indica Hybrid Rice. Vol. 42. Madison: Crop Science Society of America; 2002. pp. 766–72.
7. Peng S, Khush GS, Virk P, Tang Q, Zou Y. Progress in ideotype breeding to increase rice yield potential. Field Crops Research. 2008;108(1):32–8.
8. Liang J, Zhang J, Cao X. Grain sink strength may be related to the poor grain filling of indica-japonica rice (Oryza sativa) hybrids. Physiol Plant. 2001;112(4):470–7.

9. Mohapatra PK, Sarkar RK, Kuanar SR. Starch synthesizing enzymes and sink strength of grains of contrasting rice cultivars. Plant Sci. 2009;176(2):256–63.
10. Tsukaguchi T, Horie T, Ohnishi M. Filling Percentage of Rice Spikelets as Affected by Availability of Non-Structural Carbohydrates at the Initial Phase of Grain Filling. Japanese journal of crop science. 1996;65(3):445–52.
11. Fu J, Huang Z, Wang Z, Yang J, Zhang J. Pre-anthesis non-structural carbohydrate reserve in the stem enhances the sink strength of inferior spikelets during grain filling of rice. Field Crops Research. 2011;123(2):170–82.
12. Lemoine R, La Camera S, Atanassova R, Dédaldéchamp F, Allario T, Pourtau N, Bonnemain J-L, Laloi M, Coutos-Thévenot P, Maurousset L, et al: **Source-to-sink transport of sugar and regulation by environmental factors**. *Frontiers in Plant Science* 2013, 4(272).
13. Yang J, Peng S, Gu S, Visperas RM, Zhu Q. Changes in activities of three enzymes associated with starch synthesis in rice grains during grain filling. Zuo wu xue bao. 2001;27(2):157–64.
14. OKAWA S, MAKINO A, MAE T. Effect of Irradiance on the Partitioning of Assimilated Carbon During the Early Phase of Grain Filling in Rice. Ann Bot. 2003;92(3):357–64.
15. Morita S, Nakano H. Nonstructural Carbohydrate Content in the Stem at Full Heading Contributes to High Performance of Ripening in Heat-Tolerant Rice Cultivar Nikomaru. Crop Sci. 2011;51(2):818–28.
16. Li G, Hu Q, Shi Y, Cui K, Nie L, Huang J, Peng S. **Low Nitrogen Application Enhances Starch-Metabolizing Enzyme Activity and Improves Accumulation and Translocation of Non-structural Carbohydrates in Rice Stems**. *Frontiers in Plant Science* 2018, 9(1128).
17. Duan M, Sun SSM. Profiling the Expression of Genes Controlling Rice Grain Quality. Plant Mol Biol. 2005;59(1):165–78.
18. Ishimaru K, Hirotsu N, Madoka Y, Kashiwagi T. Quantitative trait loci for sucrose, starch, and hexose accumulation before heading in rice. Plant Physiol Biochem. 2007;45(10):799–804.
19. Samonte SOP, Wilson LT, McClung AM, Tarpley L. Seasonal Dynamics of Nonstructural Carbohydrate Partitioning in 15 Diverse Rice Genotypes. Crop Sci. 2001;41(3):902–9.
20. Nakamura Y, Yuki K, Park S-Y, Ohya T. **Carbohydrate Metabolism in the Developing Endosperm of Rice Grains**. In: *Plant and Cell Physiology*. vol. 30; 1989: 833–839.
21. Kato T. **Change of Sucrose Synthase Activity in Developing Endosperm of Rice Cultivars**. In., vol. 35; 1995: cropsci1995.0011183 × 003500030032x.
22. Braun DM, Wang L, Ruan Y-L. Understanding and manipulating sucrose phloem loading, unloading, metabolism, and signalling to enhance crop yield and food security. J Exp Bot. 2013;65(7):1713–35.
23. Beck a E, Ziegler P. Biosynthesis and Degradation of Starch in Higher Plants. Annu Rev Plant Physiol Plant Mol Biol. 1989;40(1):95–117.
24. Nielsen TH, Deiting U, Stitt M: **A [beta]-Amylase in Potato Tubers Is Induced by Storage at Low Temperature**. In., vol. 113; 1997: 503–510.
25. Preiss J. Regulation of the Biosynthesis and Degradation of Starch. In. 1982;33:431–54.

26. Jones DB, Peterson ML, Geng S. Association Between Grain Filling Rate and Duration and Yield Components in Rice1. Crop Sci. 1979;19(5):641–4.
27. Isopp H, Frehner M, Long SP, N¶sberger J: **Sucrose-phosphate synthase responds differently to source-sink relations and to photosynthetic rates**: **Lolium perenne L. growing at elevated pCO2 in the field**. In., vol. 23; 2000: 597–607.
28. Li P, Fu X, Chen M, Zhang L, Li S. Proteomic profiling and integrated analysis with transcriptomic data bring new insights in the stress responses of Kluyveromyces marxianus after an arrest during high-temperature ethanol fermentation. Biotechnol Biofuels. 2019;12:49.
29. Pan R, He D, Xu L, Zhou M, Li C, Wu C, Xu Y, Zhang W. Proteomic analysis reveals response of differential wheat (Triticum aestivum L.) genotypes to oxygen deficiency stress. BMC Genom. 2019;20(1):60.
30. Wang L, Huang Y, Wang X, Chen Y. Label-Free LC-MS/MS Proteomics Analyses Reveal Proteomic Changes Accompanying MSTN KO in C2C12 Cells. Biomed Res Int. 2019;2019:7052456.
31. Xie X, Zhao J, Xie L, Wang H, Xiao Y, She Y, Ma L. Identification of differentially expressed proteins in the injured lung from zinc chloride smoke inhalation based on proteomics analysis. Respir Res. 2019;20(1):36.
32. Xiong QQ, Shen TH, Zhong L, Zhu CL, Peng XS, He XP, Fu JR, Ouyang LJ, Bian JM, Hu LF, et al. Comprehensive metabolomic, proteomic and physiological analyses of grain yield reduction in rice under abrupt drought-flood alternation stress. Physiol Plant. 2019;167(4):564–84.
33. Ferdoushi A, Li X, Jamaluddin MFB, Hondermarck H. Proteomic Profile of Human Schwann Cells. Proteomics. 2020;20(1):e1900294.
34. Zhang Y-f, Huang X-w, Wang L-l, Wei L, Wu Z-h. You M-s, Li B-y: **Proteomic Analysis of Wheat Seed in Response to Drought Stress**. Journal of Integrative Agriculture. 2014;13(5):919–25.
35. Chen L, Chen Q, Zhu Y, Hou L, Mao P. Proteomic Identification of Differentially Expressed Proteins during Alfalfa (Medicago sativa L.) Flower Development. Front Plant Sci. 2016;7:1502.
36. Guo H, Guo H, Zhang L, Fan Y, Fan Y, Tang Z, Zeng F. **Dynamic TMT-Based Quantitative Proteomics Analysis of Critical Initiation Process of Totipotency during Cotton Somatic Embryogenesis Transdifferentiation**. *Int J Mol Sci* 2019, 20(7).
37. Li LQ, Lyu CC, Li JH, Tong Z, Lu YF, Wang XY, Ni S, Yang SM, Zeng FC, Lu LM. **Physiological Analysis and Proteome Quantification of Alligator Weed Stems in Response to Potassium Deficiency Stress**. *Int J Mol Sci* 2019, 20(1).
38. Yuan H, Chen J, Yang Y, Shen C, Xu D, Wang J, Yan D, He Y, Zheng B. Quantitative succinyl-proteome profiling of Chinese hickory (Carya cathayensis) during the grafting process. BMC Plant Biol. 2019;19(1):467.
39. Zhan Y, Wu Q, Chen Y, Tang M, Sun C, Sun J, Yu C. Comparative proteomic analysis of okra (Abelmoschus esculentus L.) seedlings under salt stress. BMC Genom. 2019;20(1):381.
40. Kim JS, Chae S, Jun KM, Pahk Y-M, Lee T-H, Chung PJ, Kim Y-K, Nahm BH. Genome-wide identification of grain filling genes regulated by the OsSMF1 transcription factor in rice. Rice.

2017;10(1):16.

41. Huang M, Zhang H, Zhao C, Chen G, Zou Y. Amino acid content in rice grains is affected by high temperature during the early grain-filling period. Sci Rep. 2019;9(1):2700.
42. Paek NC, Sexton PJ, Naeve SL, Shibles R. Differential Accumulation of Soybean Seed Storage Protein Subunits in Response to Sulfur and Nitrogen Nutritional Sources. Plant Production Science. 2000;3(3):268–74.
43. Triboï E, Martre P, Triboï-Blondel AM. Environmentally-induced changes in protein composition in developing grains of wheat are related to changes in total protein content. J Exp Bot. 2003;54(388):1731–42.
44. Gallardo K, Firnhaber C, Zuber Hln, H©richer D, Belghazi M, Henry Cl, K¼ster H, Thompson R. **A Combined Proteome and Transcriptome Analysis of Developing Medicago truncatula Seeds**. In: *Evidence for Metabolic Specialization of Maternal and Filial Tissues*. vol. 6; 2007: 2165–2179.
45. Kazłowski B, Chen M-R, Chao P-M, Lai C-C, Ko Y-T. Identification and Roles of Proteins for Seed Development in Mungbean (Vigna radiata L.) Seed Proteomes. J Agric Food Chem. 2013;61(27):6650–9.
46. Mouzo D, Bernal J, Lopez-Pedrouso M, Franco D, Zapata C. **Advances in the Biology of Seed and Vegetative Storage Proteins Based on Two-Dimensional Electrophoresis Coupled to Mass Spectrometry**. *Molecules* 2018, 23(10).
47. Fait A, Angelovici R, Less H, Ohad I, Urbanczyk-Wochniak E, Fernie AR, Galili G. Arabidopsis Seed Development and Germination Is Associated with Temporally Distinct Metabolic Switches. Plant Physiol. 2006;142(3):839–54.
48. Quinet M, Angosto T, Yuste-Lisbona FJ, Blanchard-Gros R, Bigot S, Martinez J-P, Lutts S. **Tomato Fruit Development and Metabolism**. *Frontiers in Plant Science* 2019, 10(1554).
49. Wang X, Chang L, Tong Z, Wang D, Yin Q, Wang D, Jin X, Yang Q, Wang L, Sun Y, et al. Proteomics Profiling Reveals Carbohydrate Metabolic Enzymes and 14-3-3 Proteins Play Important Roles for Starch Accumulation during Cassava Root Tuberization. Sci Rep. 2016;6:19643.

Tables

Table 1: Differentially abundant proteins involved in the identified functional protein interaction networks.

Protein accession	Regulated Type	Gene name	Subcellular localization	KEGG Gene
B8AZE9	Up	OsI_18978	chloroplast	GT; Glutathione synthase, substrate-binding, eukaryotic
A2WQ51	Down	OsI_01983	chloroplast	GST; glutathione S-transferase
A2WN71	Down	OsI_01299	chloroplast	HNRNPA1_3; heterogeneous nuclear ribonucleoprotein A1/A3
B8ALF3	Down	OsI_09682	chloroplast	RP-S17e; small subunit ribosomal protein S17e
B8B294	Up	OsI_21522	chloroplast	IBA57; transferase CAF17, mitochondrial
A2XEZ0	Up	OsI_10905	chloroplast	TR1; tropinone reductase I
A2Y4I3	Down	OsI_19910	chloroplast	XI, Xylanase inhibitor
A2WYW8	Up	OsI_05132	cytoplasm	ETF1, ERF1; peptide chain release factor subunit 1
B8B8I7	Up	OsI_25329	cytoplasm	RP-S2e; small subunit ribosomal protein S2e
B8A8Y8	Up	OsI_02167	cytoplasm	RP-L24e; large subunit ribosomal protein L24e
B8AFY2	Up	OsI_06871	cytoplasm	TAT; tyrosine aminotransferase
A2ZJS7	Up	OsI_38072	cytoplasm	glyA, SHMT; glycine hydroxymethyl transferase
A2XKG3	Down	OsI_12940	cytoplasm	DUT; dUTP pyrophosphatase
A2X2I8	Down	OsI_06407	nucleus	EIF4A; translation initiation factor 4A
B8BIC4	Up	OsI_34716	nucleus	EIF3B; translation initiation factor 3 subunit B
A2XIU7	Up	OsI_12360	nucleus	RP-L19e; large subunit ribosomal protein L19e
A2XHV1	Up	OsI_11989	nucleus	RP-L27Ae; large subunit ribosomal protein L27Ae
A2X1H8	Down	OsI_06059	nucleus	RP-L27Ae; large subunit ribosomal protein L27Ae
B8B7U0	Down	OsI_26563	mitochondria	RP-S13e; small subunit ribosomal protein S13e
A2YEZ0	Up	OsI_23687	mitochondria	GLDC; glycine dehydrogenase
B8BPG2	Up	OsI_38205	cytoskeleton	DHFR-TS; dihydrofolate reductase / thymidylate synthase
A2Y7Y4	Down	OsI_21150	extracellular	CPVL; vitellogenic carboxypeptidase-like protein

Table 2: Basic physical and chemical properties of the experimental field soil.

Soil type	pH	Organic matter (mg kg^{-1})	Avilable N (mg kg^{-1})	Avilable P (mg kg^{-1})	Avilable K (mg kg^{-1})
Clay	6.25	37.3	172	18.2	80.7

Supporting Information

TABLE S1 Detailed information about identified differentially expressed grain proteins at 3 days after full heading in rice cultivar Xiangzaoxian 42 compared to Xiangzaoxian 24.

TABLE S2 Kyoto Encyclopedia of Genes and Genomes (KEGG) functional analysis of differentially expressed proteins.

Figures

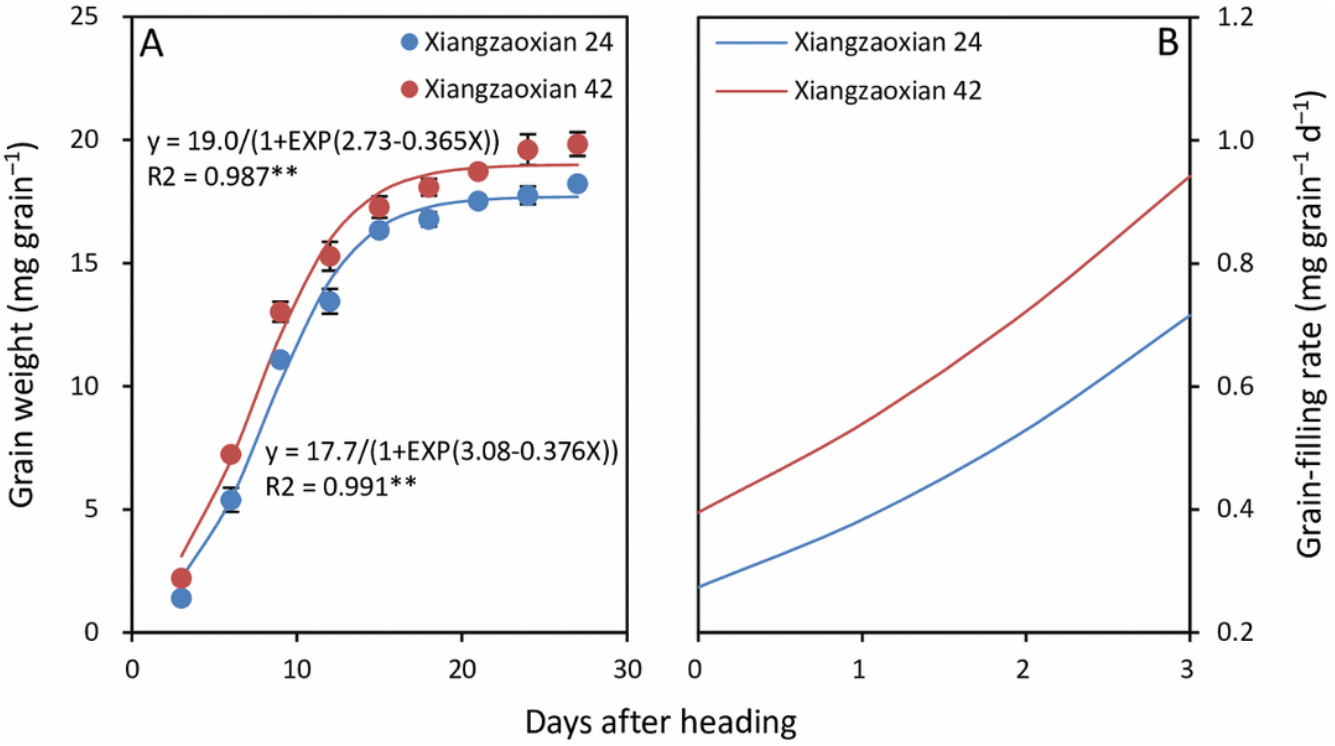

Figure 1

Grain-filling process fitted by logistic regression (A) and grain-filling rate during the period of 0–3 days after heading (B) in two rice cultivars, Xiangzaoxian 24 and Xiangzaoxian 42. In (A), data are means and SE (n = 3). ** denotes significance at the 0.01 probability level. In (B), data were calculated according to the logistic equations presented in (A).

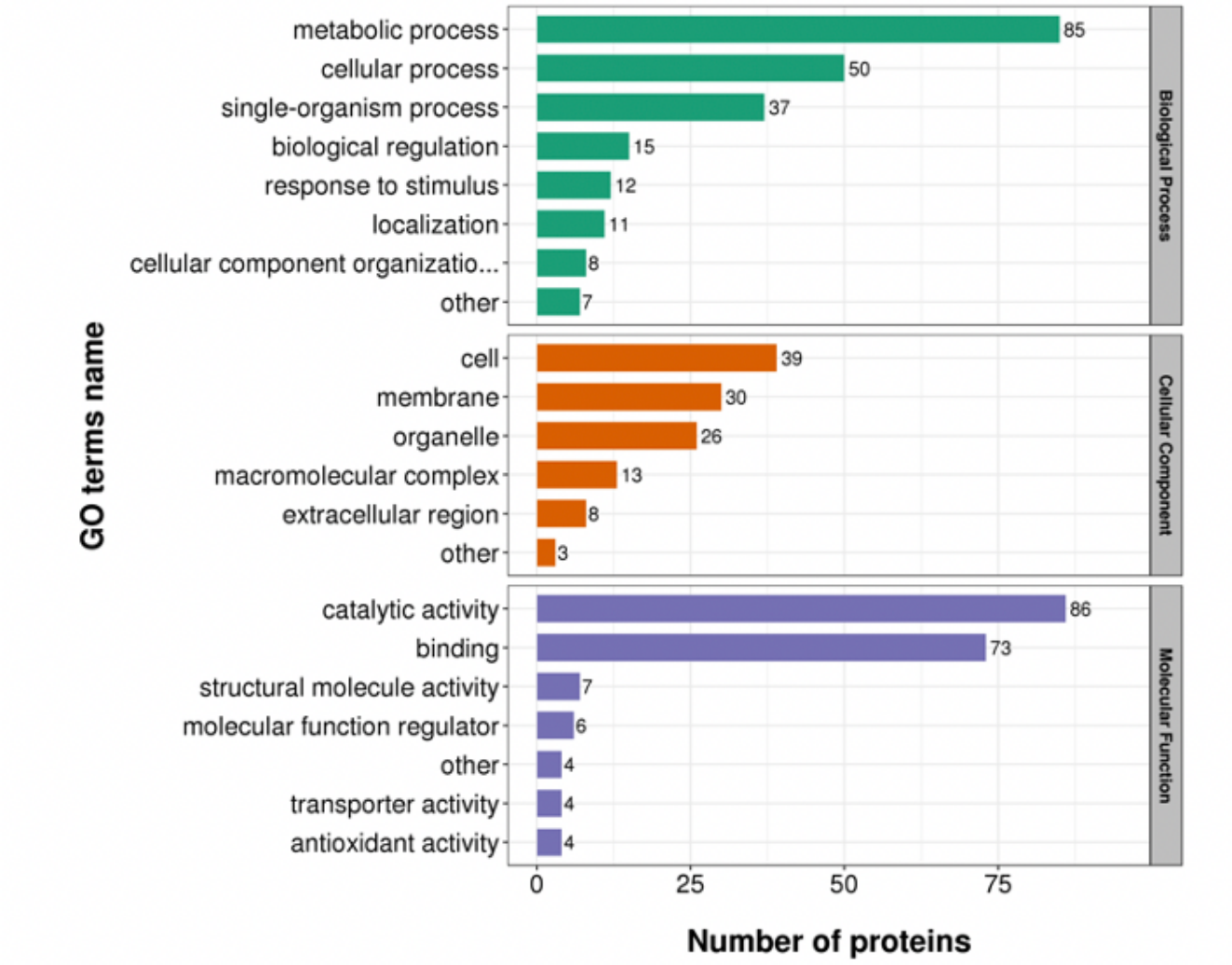

Figure 2

Statistical distribution chart of differentially expressed proteins under each GO category (2nd level).

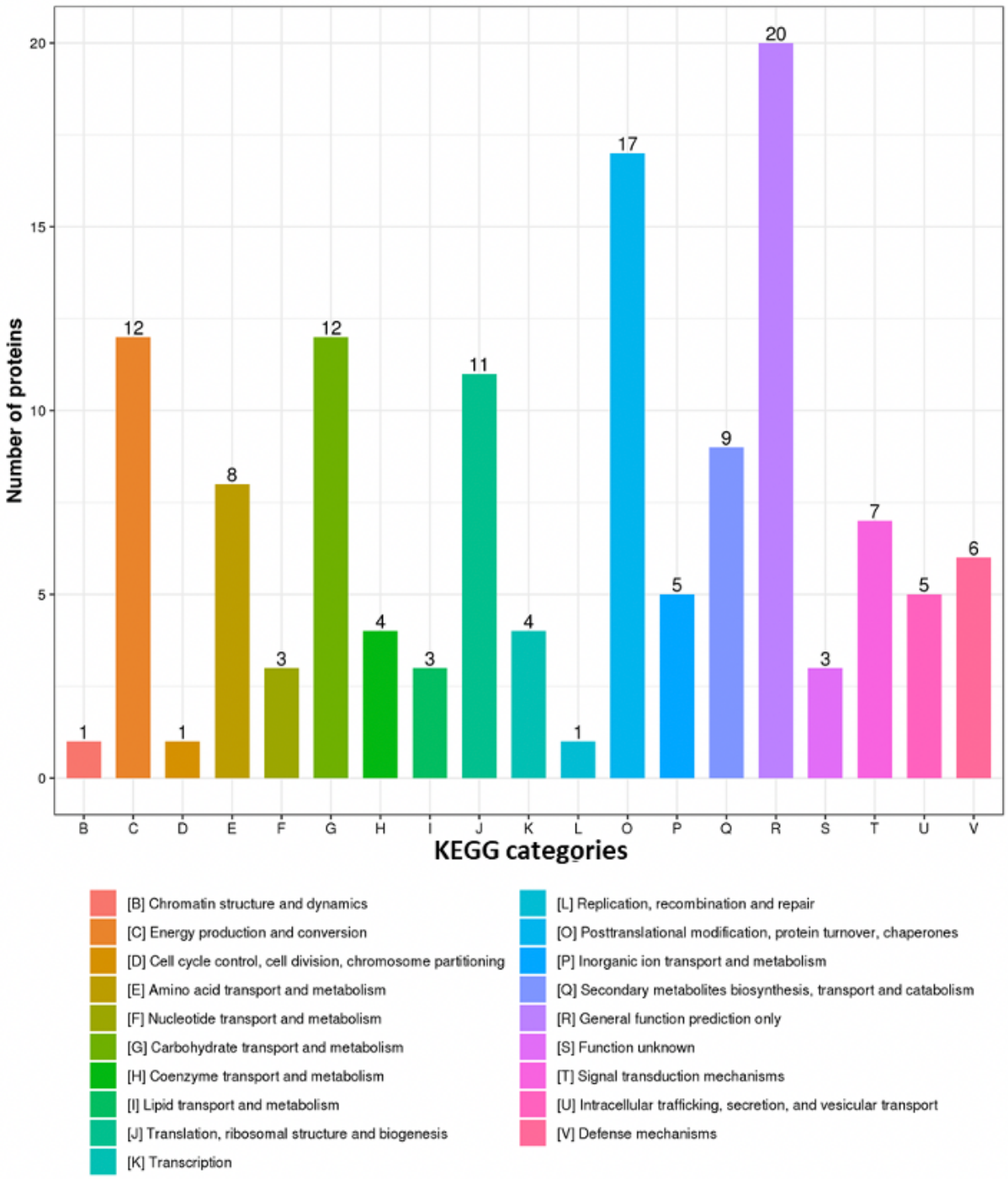

Figure 3

Kyoto Encyclopedia of Genes and Genomes (KEGG) functional classification chart of differentially expressed proteins.

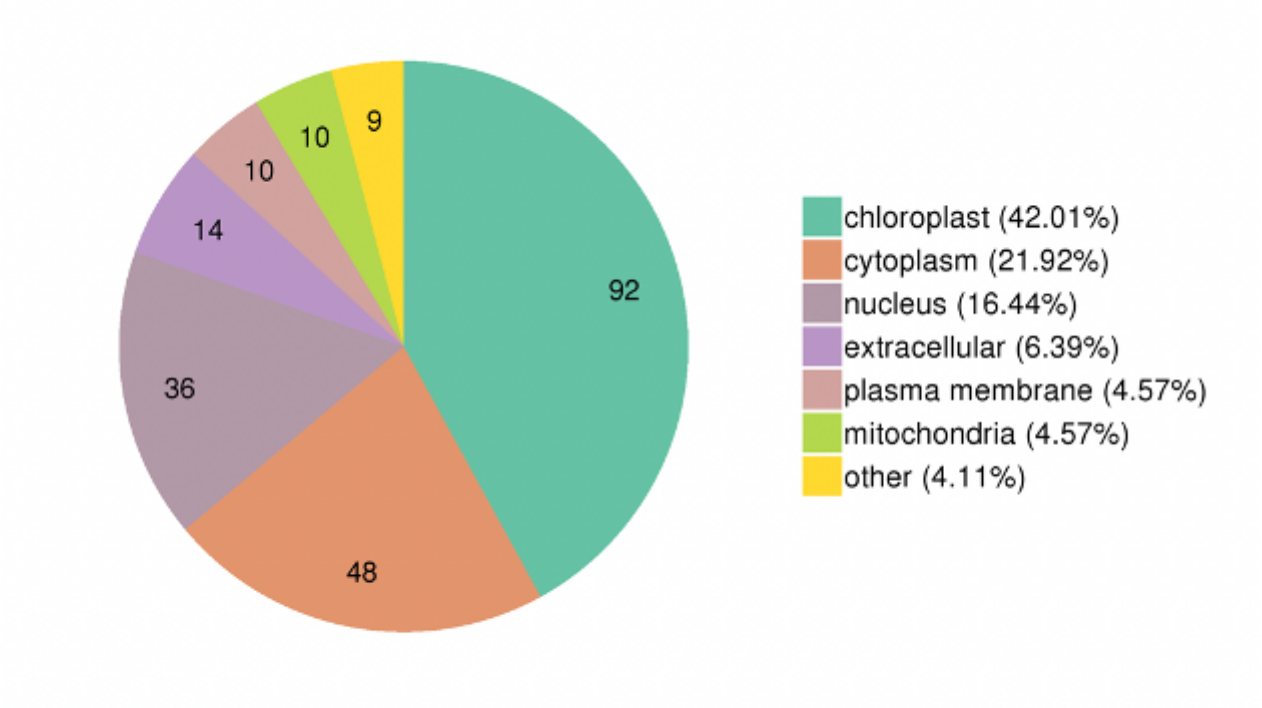

Figure 4

Subcellular localization chart of differentially expressed proteins.

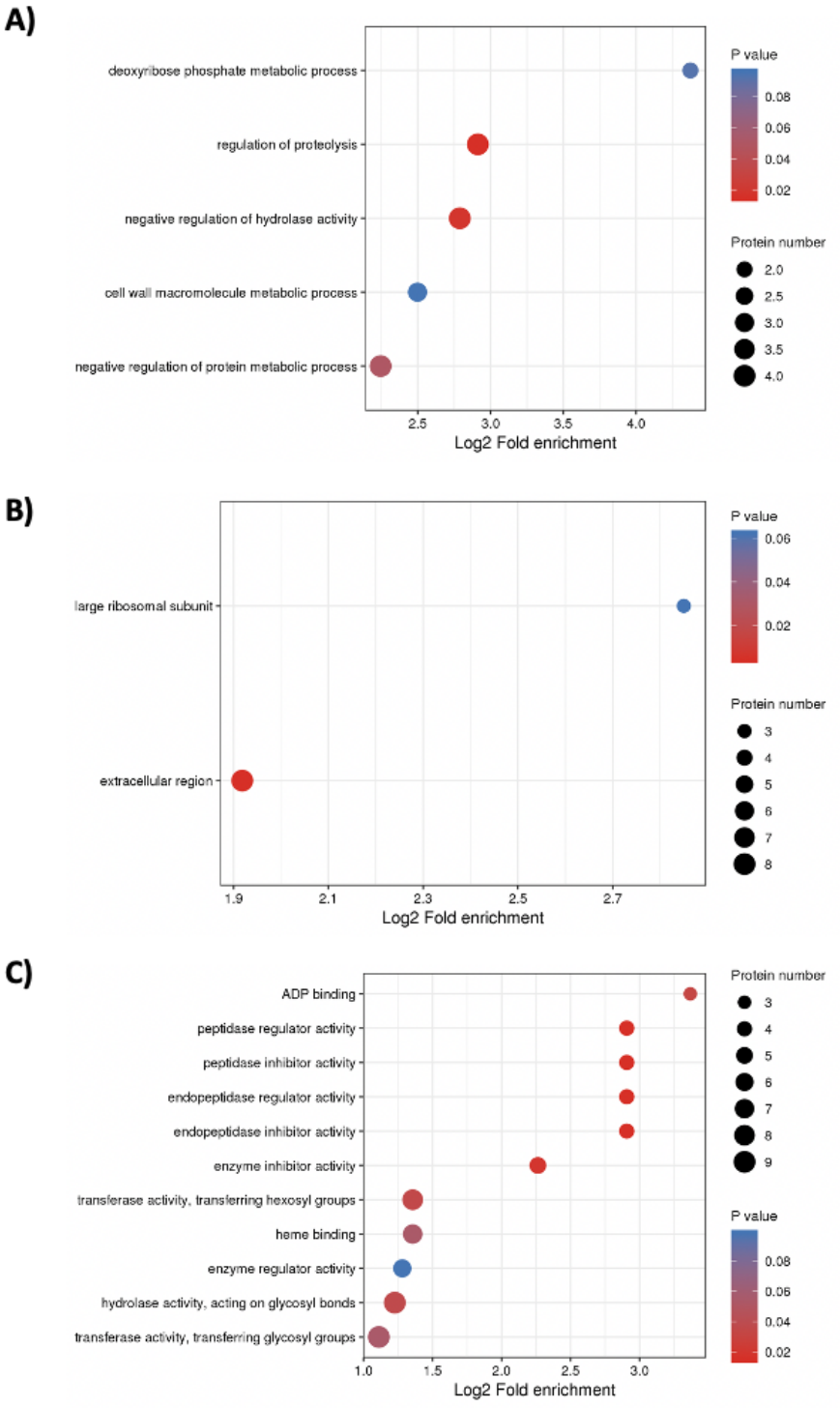

Figure 5

Gene Ontology (GO) enrichment bubble plot of differentially expressed proteins in three categories (A, biological process; B, cellular component; C, molecular function).

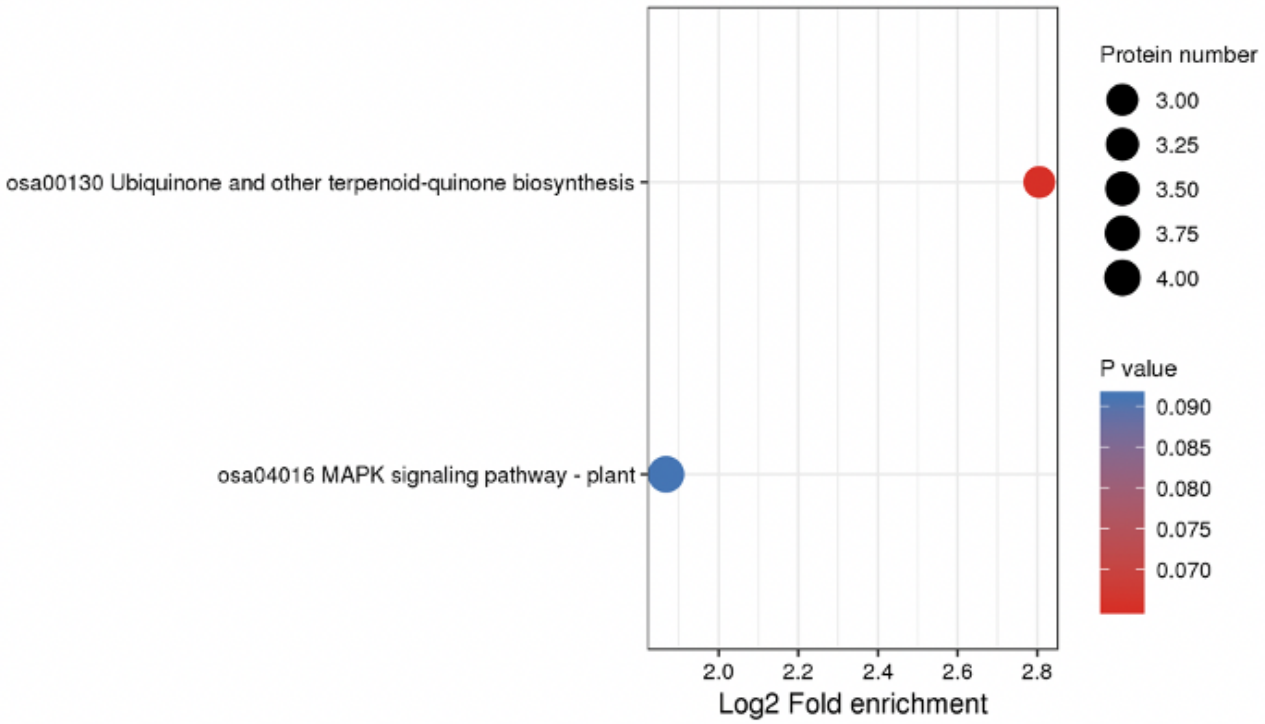

Figure 6

KEGG pathway enrichment bubble plot of differentially expressed proteins.

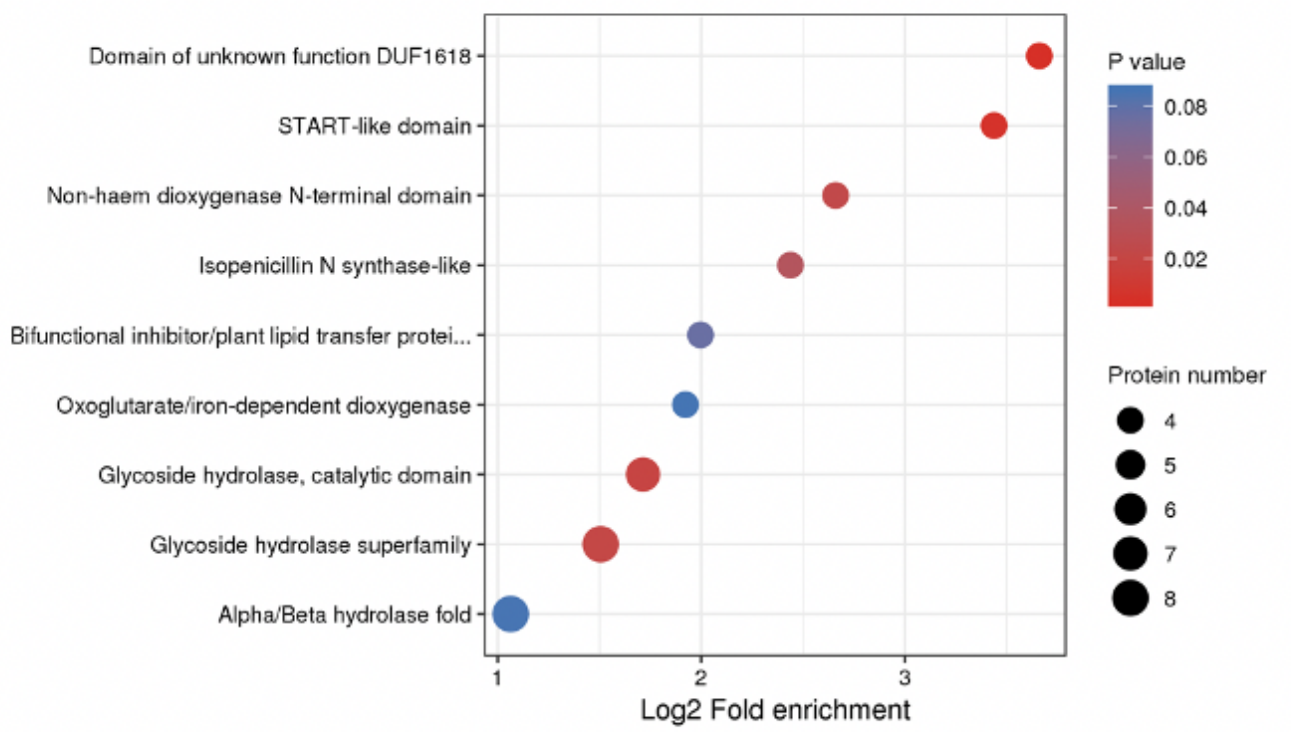

Figure 7

Protein domain enrichment bubble plot of differentially expressed proteins.

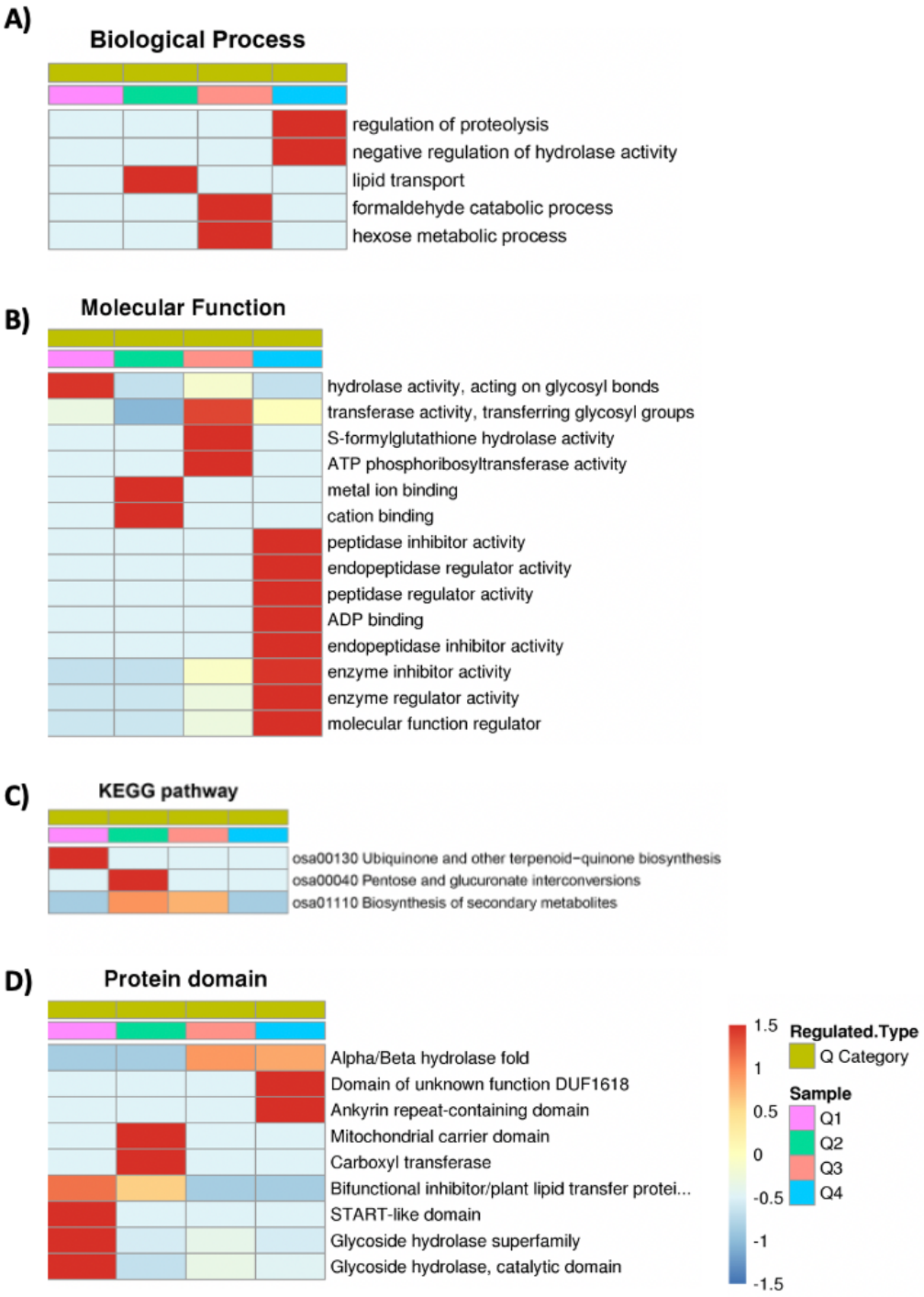

Figure 8

A comprehensive heatmap for cluster analysis of the enrichment patterns of GO functional categories, KEGG pathways and protein structural domains (A, biological process; B, molecular function; C, KEGG pathway; D, protein domain). Q1, > 1.3; Q2, 1.2–1.3; Q3, 1/1.3–1/1.2; Q4, <1/1.3.

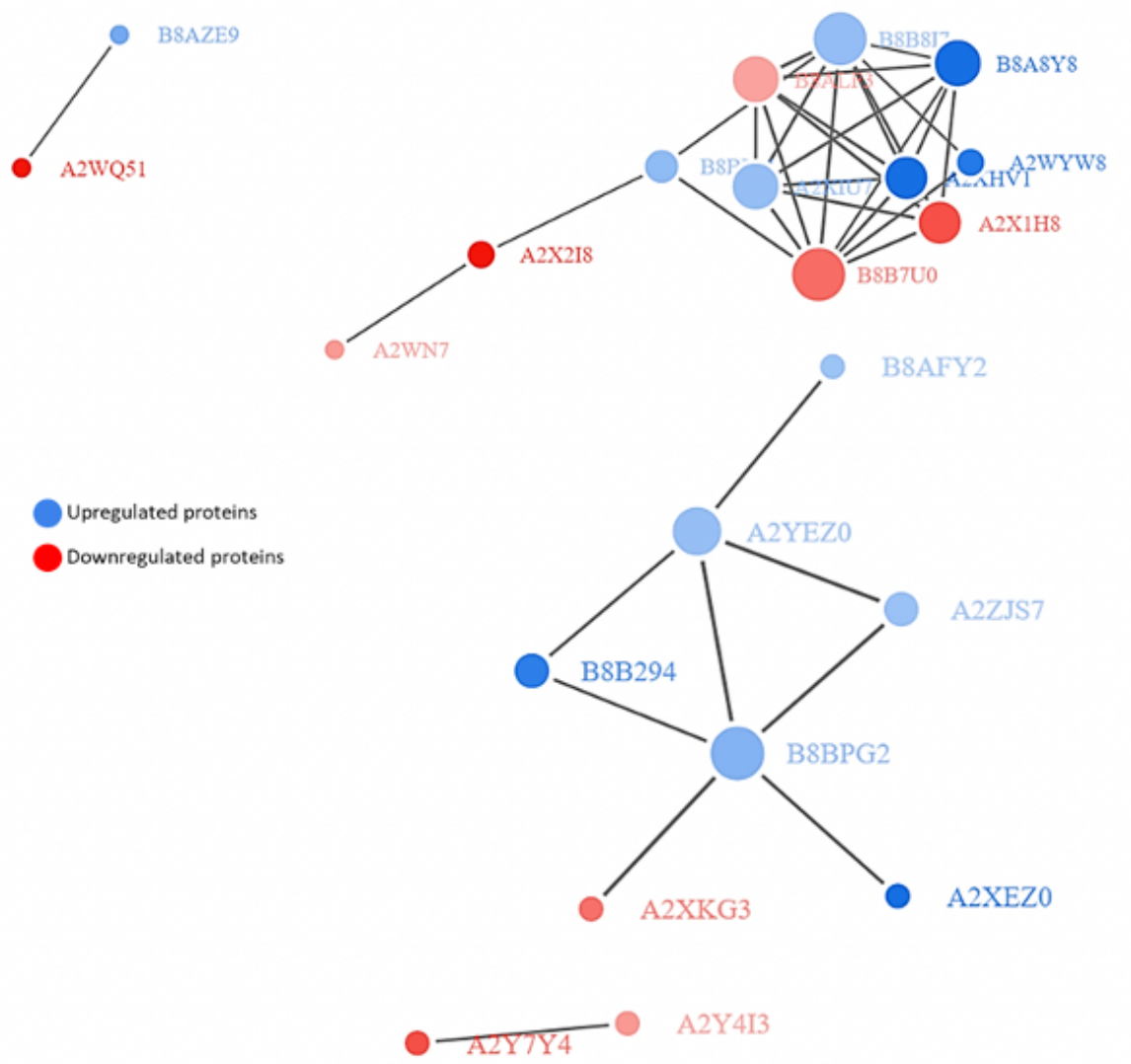

Figure 9

Functional networks of differentially abundant proteins. Note, B8AZE9; Glutathione synthase, A2WQ51; Glutathione S-transferase, A2WN71; heterogeneous nuclear ribonucleoprotein A1/A3, B8ALF3; small subunit ribosomal protein S17e, B8B294; transferase CAF17, mitochondrial, A2XEZ0; tropinone reductase I, A2Y4I3; Xylanase inhibitor, A2WYW8; peptide chain release factor subunit 1, B8B8I7; small subunit ribosomal protein S2e, B8A8Y8; large subunit ribosomal protein L24e, B8AFY2; tyrosine aminotransferase, A2ZJS7; glycine hydroxymethyl transferase, A2XKG3; dUTP pyrophosphatase, A2X2I8; ranslation initiation factor 4A, B8BIC4; translation initiation factor 3 subunit B, A2XIU7; Ribosomal protein

L19/L19e, A2XHV1; large subunit ribosomal protein L27Ae, A2X1H8; large subunit ribosomal protein L27Ae, B8B7U0; small subunit ribosomal protein S13e, A2YEZ0; glycine dehydrogenase, B8BPG2; dihydrofolate reductase / thymidylate synthase, A2Y7Y4; vitellogenic carboxypeptidase-like protein

Supplementary Files

This is a list of supplementary files associated with this preprint. Click to download.

- Supp.Table2.xlsx
- Supp.Table1.xlsx